

## Experimental Study and Distorted-Wave Predictions for the $(\text{He}^3, \alpha)$ Reaction on Fe Isotopes\*

A. G. BLAIR AND H. E. WEGNER

*Los Alamos Scientific Laboratory, University of California, Los Alamos, New Mexico*

(Received April 2, 1962)

Angular distributions of some alpha-particle groups from the  $(\text{He}^3, \alpha)$  reaction on  $\text{Fe}^{64}$ ,  $\text{Fe}^{66}$ ,  $\text{Fe}^{67}$ , and  $\text{Fe}^{68}$  have been obtained experimentally. The  $\text{He}^3$  beam energy was about 14.3 MeV except that data were also obtained for the  $\text{Fe}^{67}$  target with a beam energy of 24.9 MeV. Angular distributions were also obtained for  $\text{He}^3$  and alpha particles elastically scattered from  $\text{Fe}^{66}$ . For the  $(\text{He}^3, \alpha)$  reaction, groups corresponding to  $l=3$  neutron transfers were peaked strongly forward, while groups corresponding to  $l=1$  neutron transfers were not but showed much more diffraction structure. The cross sections for the strong  $l=3$  groups were very much larger than those for the strongest of the  $l=1$  groups. This ratio is in distinct contrast to the results of  $(d, t)$  and  $(p, d)$  experiments on the same isotopes. In addition, the  $\text{Fe}^{67}(\text{He}^3, \alpha)$  reaction to the ground and first-excited states of  $\text{Fe}^{66}$  proceeded with a cross section lower by more than an order of magnitude than

that expected on the basis of data from the  $(d, t)$  and  $(p, d)$  reactions.

The  $(\text{He}^3, \alpha)$  reaction cannot be satisfactorily analyzed with the plane-wave Butler-Born calculation. In contrast, the distorted-wave Born-approximation calculation predicts curves which are usually in good agreement with the experimental angular distributions, and yields ratios of spectroscopic factors which are in fair to good agreement with the results of a plane-wave analysis of the  $(d, t)$  data and in fair agreement with the results of a distorted-wave analysis of the  $(p, d)$  data. The parameter values used in the distorted-wave calculation for the  $(\text{He}^3, \alpha)$  reaction on  $\text{Fe}^{64}$ ,  $\text{Fe}^{66}$ , and  $\text{Fe}^{68}$  were very nearly those which yielded the best optical-model fits to the  $\text{Fe}^{66}$  elastic scattering data. The distorted-wave calculation for the  $\text{Fe}^{67}(\text{He}^3, \alpha)\text{Fe}^{66}$  reaction required somewhat different parameter values.

### I. INTRODUCTION

IN the past several years a large number of  $(d, t)$  reaction experiments and several  $(p, d)$  experiments have been reported in the literature.<sup>1</sup> The angular distributions obtained in these experiments usually show typical direct-interaction stripping patterns for incident-particle energies in the region from 5 to 20 MeV. A great amount of spectroscopic and nuclear information has been obtained by the technique of fitting plane-wave Butler-Born approximation (PW) curves to the angular distributions and extracting angular-momentum  $l$ -transfer values and reduced widths.<sup>1</sup> More recently, digital computer codes which perform distorted-wave Born-approximation (DW) calculations have become available,<sup>2-4</sup> and the calculations have been applied to  $(d, p)$  stripping distributions with considerable success.<sup>5,6</sup> No application of DW calculations to  $(d, t)$  reaction distributions has yet appeared in the literature, although some  $(p, d)$  distributions have been fitted.<sup>7</sup>

A reaction which should in many ways be analogous to the  $(d, t)$  or  $(p, d)$  pickup reactions is the  $(\text{He}^3, \alpha)$  reaction. Many experiments on the  $(\text{He}^3, \alpha)$  reaction have been reported at  $\text{He}^3$  energies of 10 MeV and below,

and the results generally show angular distributions characteristic of direct-interaction processes. However, PW analyses of the  $(\text{He}^3, \alpha)$  reaction are in general less fruitful than those of  $(d, t)$  or  $(p, d)$  reactions, owing to the following characteristics:

(1) As in  $(d, t)$  analyses, a reduced width  $\theta^2$  cannot be directly extracted from PW fits to the  $(\text{He}^3, \alpha)$  reaction data; only a number  $\Theta^2$ , given by

$$\Theta^2 = C^2 \Lambda \theta^2, \quad (1)$$

can be determined.<sup>1</sup> In Eq. (1),  $C^2$  is an isotopic-spin coupling factor, and  $\Lambda$  is a number related, in part, to the overlap between the incoming- and outgoing-particle internal wave functions. In practice,  $\Lambda$  is determined empirically. The reduced width  $\theta^2$  can be written as

$$\theta^2 = S \theta_0^2, \quad (2)$$

where  $S$  is the spectroscopic (nuclear overlap) factor, and  $\theta_0^2$  is the single-particle reduced width, the value of which can be determined empirically from  $(d, p)$  and  $(p, d)$  reactions on appropriate nuclei. The factor  $\theta_0^2$  includes a simulation of the distortion effects neglected by the PW theory in the  $(d, p)$  or  $(p, d)$  reactions, and therefore depends not only on  $l$  transfer, but to some extent on two other parameters, energy and target.<sup>1,8</sup> For other reactions, such as  $(d, t)$  and  $(\text{He}^3, \alpha)$ , the distortion effects will be different; if values of  $\theta_0^2$  determined from  $(d, p)$  and  $(p, d)$  reactions are used in the analysis of these other reactions,  $\Lambda$  will contain the effect of these differences in distortion in addition to the particle overlap. For the  $(d, t)$  reaction,  $\Lambda$  is known fairly well for nuclei in the mass region of  $A \lesssim 60$ , and reliable reduced-width information may therefore be

\* Work performed under the auspices of the U. S. Atomic Energy Commission.

<sup>1</sup> M. H. Macfarlane and J. B. French, *Revs. Modern Phys.* **32**, 567 (1960).

<sup>2</sup> W. Tobocman, *Phys. Rev.* **115**, 98 (1959).

<sup>3</sup> R. H. Bassel, R. M. Drisko, and G. R. Satchler, Oak Ridge National Laboratory Report-3240 (unpublished).

<sup>4</sup> B. Buck and P. E. Hodgson, *Phil. Mag.* **71**, 1371 (1961).

<sup>5</sup> B. L. Cohen, R. H. Fulmer, and A. L. McCarthy, *Bull. Am. Phys. Soc.* **7**, 81 (1962); E. D. Scott, *Nuclear Phys.* **27**, 490 (1961); D. H. Wilkerson, *Proceedings of the International Conference on Nuclear Structure, Kingston* (University of Toronto Press, Toronto, 1960), pp. 36-46.

<sup>6</sup> D. W. Miller, H. E. Wegner, and W. S. Hall (to be published).

<sup>7</sup> C. D. Goodman, J. B. Ball, and C. B. Fulmer (to be published).

<sup>8</sup> M. H. Macfarlane, B. J. Raz, J. L. Yntema, and B. Zeidman (to be published).

obtained from the data. In the case of the  $(\text{He}^3, \alpha)$  reaction, however,  $\Lambda$  is completely undetermined, and reduced widths cannot be obtained from the data. It is possible, in fact, that the parameter dependence of  $\Lambda$  for the two reactions is so different that not even ratios of the factor  $\Lambda\theta^2$  obtained from the PW analysis of  $(\text{He}^3, \alpha)$  reaction data can be compared to ratios from the  $(d, t)$  data for the same nuclear transitions, except under certain restricted conditions.

(2) The  $Q$  of a  $(\text{He}^3, \alpha)$  reaction to the ground state of the final nucleus is, with exceptions particularly at closed-shell nuclei, about 9 MeV or greater. The kinematics of the reaction are then such that, for  $\text{He}^3$  energies of approximately 15 MeV and higher, the usual first maximum of angular distributions for  $l \leq 2$  does not appear, and even  $l=3$  distributions typically peak at  $\theta \approx 10^\circ$ . It is not possible to extract reliable values of reduced widths from PW fits to angular distributions that lack the usual first maximum.

(3) Both the incoming and emerging particles are doubly charged in a  $(\text{He}^3, \alpha)$  reaction. Hence, at a higher energy and for a lower target atomic number than for a comparable  $(d, t)$  or  $(p, d)$  reaction, the Coulomb potential experienced by these particles becomes a dominant factor in the reaction.

A DW analysis should correct for the PW limitations mentioned above and, hence, should be a valid description of the  $(\text{He}^3, \alpha)$  reaction. It is important to note, however, that the DW calculations cannot at present predict absolute cross sections for this reaction. This limitation is in part due to approximations made in the calculations. Furthermore, the overlap integral between the  $\text{He}^3$  and the alpha particle internal wave functions is not known. Therefore, only ratios of spectroscopic factors can be calculated.

In order to apply DW calculations to a particular reaction, parameter values obtained from optical model fits to the appropriate elastic scattering data are required. In the present experiment, the choice of 14.5 MeV as the  $\text{He}^3$  beam energy was thus partly dictated by the fact that the reaction alpha particles would then have energies within the operating range of the Los Alamos variable-energy cyclotron.

The choice of the Fe isotopes as targets was prompted by the publication of the results of  $(d, t)$  experiments by Zeidman *et al.*<sup>9</sup> and Macfarlane *et al.*<sup>8</sup> on some  $A \approx 60$  nuclides, including the Fe isotopes. In addition, Goodman *et al.*<sup>7</sup> have recently performed a  $(p, d)$  experiment on the Fe isotopes. Strong  $l=1$  and  $l=3$  transitions occur in these reactions, and many of the final levels are separated sufficiently to permit resolution with our equipment.

The main objectives of the present experiment were, first, to compare the systematics of the angular distributions from the  $(\text{He}^3, \alpha)$  reaction on  $\text{Fe}^{56}$  and  $\text{Fe}^{57}$  with

the  $(d, t)$  and  $(p, d)$  distributions from these isotopes and, second, to examine the applicability of DW calculations in the fitting of the  $(\text{He}^3, \alpha)$  angular distributions and prediction of ratios of spectroscopic factors. Angular distributions from the  $(\text{He}^3, \alpha)$  reaction on the isotopes  $\text{Fe}^{54}$  and  $\text{Fe}^{58}$  were also obtained, but no effort was made to determine the appropriate parameter values required for DW calculations. During the course of the experiment, some of the  $(d, t)$  measurements made by the Argonne group<sup>8,9</sup> were repeated at a deuteron energy of 14 MeV.

## II. EXPERIMENTAL PROCEDURE

$\text{He}^3$  particles, accelerated to 14.5 MeV in the Los Alamos variable-energy cyclotron, were focussed as a  $\frac{1}{16} \times \frac{5}{32}$ -in. vertical beam spot on a target in a remote, 10-in.-diam scattering chamber. The details of the scattering chamber, counter support, and scattering geometry have been described previously.<sup>10</sup> For a 14.5-MeV  $\text{He}^3$  beam energy, alpha particles from the  $(\text{He}^3, \alpha)$  reaction on Fe isotopes have energies up to approximately 27 MeV. At these energies,  $\text{He}^3$  and alpha particles can be detected with commercially available semiconductor detectors, which have the property of providing energy resolution superior to that obtained with NaI crystal-photomultiplier systems. The measurements were made with  $p$ - $n$  junction detectors,<sup>11</sup> and with Au surface barrier detectors.<sup>12</sup>

It is important that the depletion depth of the semiconductor detector be thick enough that the most energetic alpha particles will stop within it; otherwise the spectra will be distorted. The depletion depth was tested with the aid of the  $\text{Be}^9(\text{He}^3, \alpha)\text{Be}^8$  reaction, whose ground-state  $Q$  is 18.9 MeV. Observation of the  $\text{Be}^8$  ground-state alpha particles at different forward angles showed the depletion depth to be adequate for the measurements on the Fe isotopes.

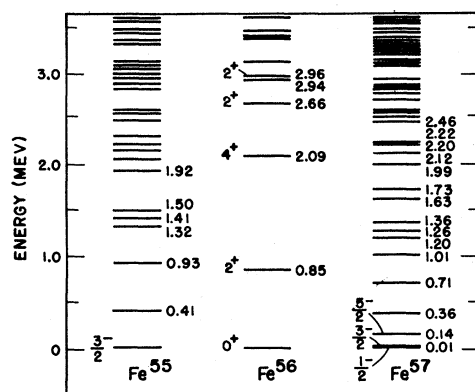
At small scattering angles ( $\theta \lesssim 30^\circ$ ), the  $\text{He}^3$  particles elastically scattered from the Fe targets produce a pulse pileup in the electronic system unless the beam current is kept extremely low. For these angles, absorber foils which were thick enough to stop the elastically scattered  $\text{He}^3$  particles, but which allowed the higher energy alpha particles from the  $(\text{He}^3, \alpha)$  reaction to penetrate, were placed in front of the detectors. However, a small fraction of the absorbed  $\text{He}^3$  particles reacts with the absorber material to produce protons, deuterons, and tritons that may penetrate the rest of the absorber and be detected. At some small angle ( $\theta \approx 5^\circ$ ), therefore, the technique fails; the number of secondary particles is so large as to again produce an electronic pileup. Platinum foil was used for the ab-

<sup>10</sup> H. E. Wegner and W. S. Hall, Phys. Rev. **119**, 1654 (1960).

<sup>11</sup> Guard ring-type detector,  $p$ - $n$  junction, 4000  $\Omega$ -cm, Solid State Radiations, Inc., 2261 So. Carmelina, Los Angeles 64, California.

<sup>12</sup> Gold surface barrier detector, 3200  $\Omega$ -cm, Oak Ridge Technical Enterprises Corp., P. O. Box 524, Oak Ridge, Tennessee.

<sup>9</sup> B. Zeidman, J. L. Yntema, and B. J. Raz, Phys. Rev. **120**, 1723 (1960).

FIG. 1. Energy-level structure of  $\text{Fe}^{55}$ ,  $\text{Fe}^{56}$ , and  $\text{Fe}^{57}$ .

sorber to minimize this effect, since the Coulomb barrier suppresses the  $\text{He}^3$ -induced reactions.

When the  $(\text{He}^3, \alpha)$  reaction  $Q$  was low, or when the reaction was observed at back angles, the alpha-particle energy from the reaction on the targets was small. For such cases, a mass-discrimination detector system was used to discriminate against reaction protons and deuterons of comparable energies. A parallel-plate ionization chamber measured  $\Delta E$ , the energy lost by the detected particle in passing through the chamber. One of the semiconductor detectors described previously was used to detect the residual energy of the particle,  $E$ , after its penetration of the  $\Delta E$  chamber. The details of the mass-discrimination detector system are described elsewhere.<sup>13</sup>

Because we observed an unusually low cross section for the  $\text{Fe}^{57}(\text{He}^3, \alpha)\text{Fe}^{56}$  reaction, as compared to the previously reported  $\text{Fe}^{57}(d, t)\text{Fe}^{56}$  reaction at 20 MeV,<sup>9</sup> we investigated the  $(d, t)$  reaction on  $\text{Fe}^{56}$ ,  $\text{Fe}^{57}$ , and  $\text{Fe}^{58}$  for 14-MeV deuterons. These measurements were made with the mass-discrimination detector system described in the previous paragraph, in which a Au surface barrier detector<sup>12</sup> was employed as the  $E$  detector. This unit was constructed of 3200- $\Omega$ -cm  $n$ -type silicon and was operated at a bias of 380 V. Under these conditions, the depth of the depletion region of the detector was greater than the maximum range of the detected tritons.<sup>1</sup>

The over-all energy resolution of the detector systems was approximately 1.5% or less (full width at half-maximum), but cyclotron energy fluctuations, beam energy spread, and occasional electronic instabilities resulted in an operational energy resolution of 2 to 3%.

The energies of the detected particles were recorded on a multi-channel analyzer. The resulting spectra were analyzed with a computer code which fits a Gaussian curve to each of the peaks corresponding to an observed level or group of levels, determines the area under the curve, and computes the corresponding cross section. The code is capable of unfolding partially resolved

peaks superimposed on various types of backgrounds. The data reduction method is described in detail elsewhere.<sup>14</sup>

Thin, self-supporting target foils of  $\text{Fe}^{56}$ ,  $\text{Fe}^{57}$ , and  $\text{Fe}^{58}$  were produced by electroplating,<sup>15</sup> and the  $\text{Fe}^{54}$  target by rolling methods. The areal densities ranged from 1 to 3 mg/cm<sup>2</sup>; the isotopic purity varied from 78 to 99%, depending on the particular isotope.

The angular distributions reported here were measured several times with different detector systems in order to test the reproducibility of the data and obtain cross checks on the various absolute and relative cross sections. Under some conditions, the detector solid angle could not be accurately calculated because of multiple Coulomb scattering, but all data measured under such conditions were normalized to data measured under known solid-angle conditions.

### III. RESULTS

A partial compilation of the energy levels of  $\text{Fe}^{55}$ ,  $\text{Fe}^{56}$ , and  $\text{Fe}^{57}$  and their known spins and parities is shown in Fig. 1.<sup>16</sup> For  $\text{Fe}^{54}$  and  $\text{Fe}^{58}$ , only the  $0^+$  ground states are involved in the reactions to be discussed, and hence the level diagrams for these isotopes are not shown. Although gross structure groups observed for the levels of  $\text{Fe}^{55}$  will be discussed, the energy resolution was inadequate to determine the exact nature of the groups of levels, and a level diagram is not included.

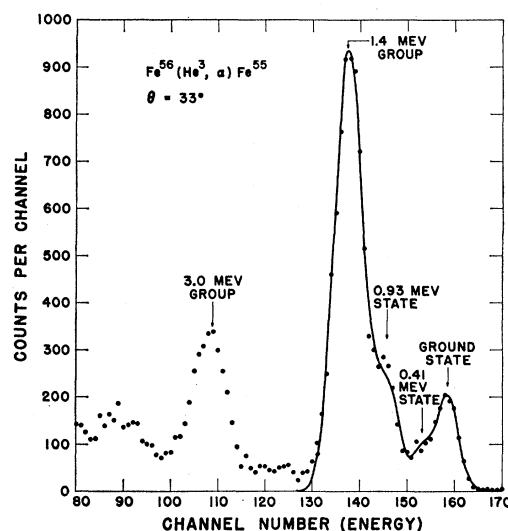


FIG. 2. Energy spectrum of alpha particles from the  $\text{Fe}^{56}(\text{He}^3, \alpha)\text{Fe}^{55}$  reaction at  $\theta_{\text{lab}} = 33^\circ$ . The curve through the datum points is the best fit computed by the data analysis code.

<sup>14</sup> P. T. McWilliams, W. S. Hall, and H. E. Wegner, *Rev. Sci. Instr.* **33**, 70 (1962).

<sup>15</sup> We are indebted to R. Seegmiller of this Laboratory for the preparation of these targets.

<sup>16</sup> K. Way *et al.*, *Nuclear Data Sheets*, National Academy of Sciences, National Research Council (U. S. Government Printing Office, Washington, D. C.).

<sup>13</sup> H. E. Wegner (to be published).

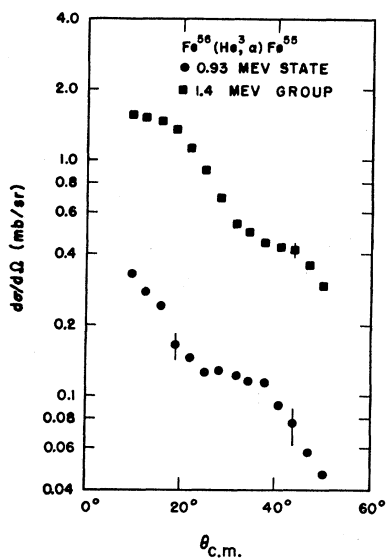


FIG. 3. Angular distributions for the  $\text{Fe}^{56}(\text{He}^3, \alpha)\text{Fe}^{55}$  reaction to the 0.93-MeV state and the 1.4-MeV group. The error bars indicate the variation in relative cross sections obtained under different analysis procedures.

#### A. $\text{Fe}^{56}(\text{He}^3, \alpha)\text{Fe}^{55}$ Reaction

The ground state  $Q$  for the  $\text{Fe}^{56}(\text{He}^3, \alpha)\text{Fe}^{55}$  reaction is 9.37 MeV.<sup>17</sup> A typical energy spectrum for alpha particles from this reaction at a laboratory scattering angle of  $33^\circ$  is shown in Fig. 2. The peaks are labeled in accordance with the level diagram shown in Fig. 1. The levels that comprise the 1.4-MeV and 3.0-MeV groups are not resolved, and each group is analyzed as though it were a single level. The peaks corresponding to these two groups maintained a Gaussian-like shape throughout the entire angular distribution and could be analyzed in a reasonably consistent fashion.

Although the peaks corresponding to the ground-, first-excited, and second-excited states and the 1.4-MeV group were analyzed separately, the resulting angular distributions sometimes showed considerable scattering of datum points. This effect reflects the difficulty in obtaining a consistent analysis of the spectra with the available statistics and energy stability during the measurements. The beam energy and spread underwent small changes during a measurement at a particular scattering angle; these changes distorted the spectrum slightly, which in turn resulted in less reliable individual peak analyses. An example of the angular distributions obtained is shown in Fig. 3. The two distributions shown have approximately the same shapes, but the details of the distribution of the relatively weakly excited 0.93-MeV state are not so clear as those of the 1.4-MeV group. The ground- and first-excited state distributions behave similarly.

Owing to the difficulty in unfolding the ground-state distribution from the first-excited state distribution, and the second-excited state distribution from the 1.4-MeV group distribution, the distributions were added

together in pairs as shown in Fig. 4. The reliability of the datum points is increased considerably by this pairing. Also shown in the figure is the angular distribution of the 3.0-MeV group.

Because the ground state of  $\text{Fe}^{55}$  has a spin and parity of  $\frac{3}{2}^-$  and the first-excited state is  $\frac{1}{2}^-$  or  $\frac{3}{2}^-$ ,<sup>9</sup> and since the  $\text{Fe}^{56}$  ground-state spin and parity is  $0^+$ , the angular momentum transfer to both levels must be  $l=1$ . The angular distribution of this group shows considerable oscillatory structure with a modest increase in cross section in the forward angle region.

The 1.4-MeV group transition was observed to be a mixture of  $l=1$  and  $l=3$  in the  $(d, t)$  experiment of Zeidman *et al.*<sup>9</sup> but was predominantly  $l=3$  in terms of the reduced widths. As will be discussed below,  $l=3$  transitions are enhanced over  $l=1$  transitions in the  $(\text{He}^3, \alpha)$  reaction, so that to a good approximation the  $(\text{He}^3, \alpha)$  transitions to the 1.4-MeV group of  $\text{Fe}^{55}$  show a pure  $l=3$  character. The transition to any single  $\text{Fe}^{55}$  level can involve only a single  $l$  value, and it is clear from inspection of Fig. 3 that the transition to the 0.93-MeV state of  $\text{Fe}^{55}$  is  $l=3$ . The spin and parity of the 0.93-MeV state is thus  $\frac{5}{2}^-$  or  $\frac{7}{2}^-$ .

The sum distribution of the 0.93-MeV state and 1.4-MeV group, as shown in Fig. 4, thus shows a nearly pure  $l=3$  character. This distribution is strongly peaked forward and shows less oscillatory structure than the  $l=1$  ground- and first-excited state distribution. The cross section of the 0.93- and 1.4-MeV group of transitions is greater than that of the ground group throughout the entire angular distribution and more than ten

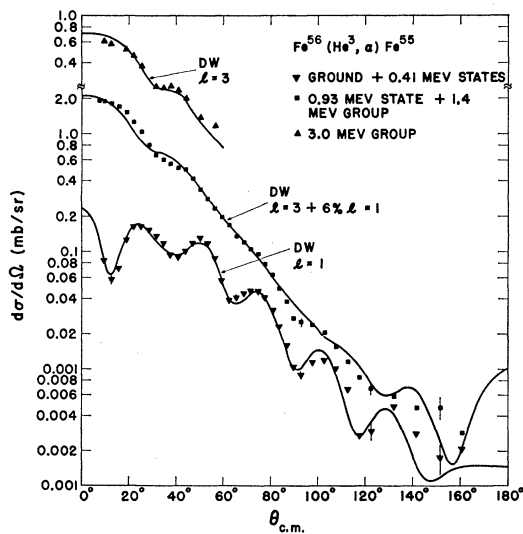


FIG. 4. Angular distributions for the  $\text{Fe}^{56}(\text{He}^3, \alpha)\text{Fe}^{55}$  reaction to the ground and 0.41-MeV states, 0.93- and 1.4-MeV group, and 3.0-MeV group. The laboratory energy of the  $\text{He}^3$  beam was  $14.40 \pm 0.15$  MeV. The solid lines result from DW calculations arbitrarily normalized to the data. The parameter values used in the calculations are, for the  $\text{He}^3$  well,  $V = -32$  MeV,  $W = -13$  MeV,  $R = 6.4$  F,  $a = 0.58$  F; for the alpha well,  $V = -79$  MeV,  $W = -12$  MeV,  $R = 5.8$  F,  $a = 0.60$  F; and for the neutron well,  $R_N = 6.9$  F.

<sup>17</sup> All  $Q$  values are taken from V. J. Ashby and H. C. Catron, University of California Radiation Laboratory Report-5419, 1959 (unpublished).

times greater in the forward-angle region. This result is in distinct contrast to the results of the  $(d, t)^9$  and  $(p, d)^7$  experiments, and will be discussed in detail later. The backward-angle region of the distributions was only partially investigated because the cross section is only a few microbarns; operational limitations prevented further measurements.

The strength of the 3-MeV-group angular distribution and its similarity to the 1.4-MeV-group distribution indicates strong  $l=3$  transitions to a state or states within the group.

For all angular distributions shown in this paper, the representative error bars on the datum points indicate the relative cross section errors, including statistics and background. For the angular distributions for which no error bars are shown, the errors are smaller than the dimensions of the datum points. The absolute cross sections (in the c.m. system) were determined to an accuracy of  $\pm 15\%$ . This error was determined from a consideration of the uniformity of the targets and the over-all reproducibility of the data.

The incident-particle energy indicated in the caption of each angular-distribution figure is the average energy at the center of the target. The indicated variation is the limit to which the energy was held through the course of a complete angular-distribution measurement.

The angular acceptance of the detector systems varied from  $1^\circ$  to  $2^\circ$ , depending on the particular geometry employed.

### B. $\text{Fe}^{57}(\text{He}^3, \alpha)\text{Fe}^{56}$ Reaction

The ground-state  $Q$  of the  $\text{Fe}^{57}(\text{He}^3, \alpha)\text{Fe}^{56}$  reaction is 12.94 MeV. The energy distribution for alpha particles from this reaction at a laboratory scattering angle of  $33^\circ$  is shown in Fig. 5. The ground- and first-

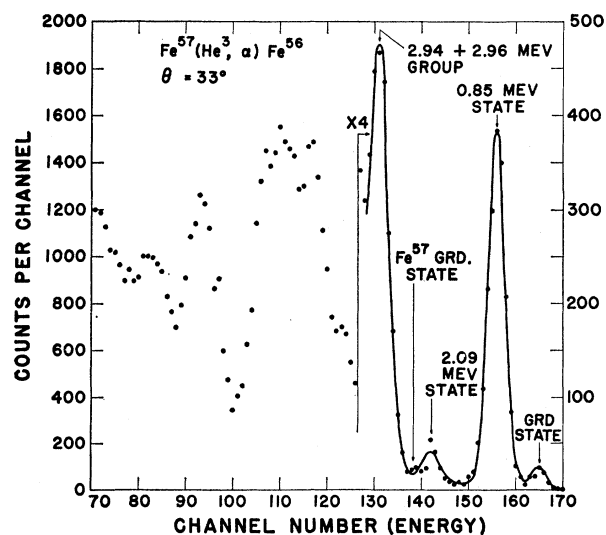


FIG. 5. Energy spectrum of alpha particles from the  $\text{Fe}^{57}(\text{He}^3, \alpha)\text{Fe}^{56}$  reaction at  $\theta_{\text{lab}} = 33^\circ$ . Note the change in ordinate scale at channel No. 127. The curve through the datum points is the best fit computed by the data analysis code.

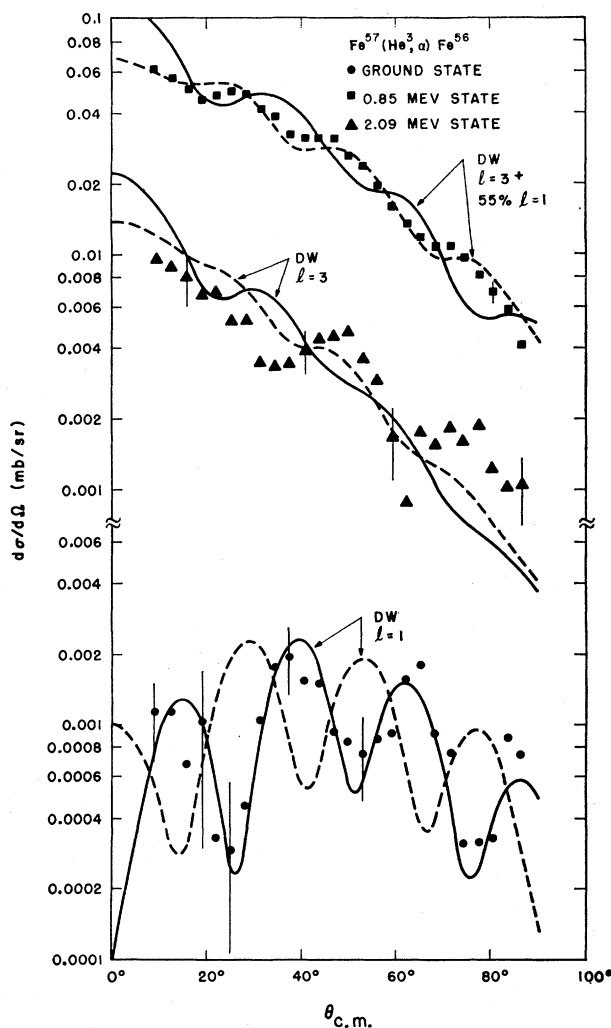


FIG. 6. Angular distributions for the  $\text{Fe}^{57}(\text{He}^3, \alpha)\text{Fe}^{56}$  reaction to the ground, 0.85-MeV, and 2.09-MeV states. The laboratory energy of the  $\text{He}^3$  beam was  $14.30 \pm 0.15$  MeV. The solid lines result from DW calculations in which the parameter values were, for the  $\text{He}^3$  well,  $V = -32$  MeV,  $W = -13$  MeV,  $R = 6.45$  F,  $a = 0.58$  F; for the alpha well,  $V = -85$  MeV,  $W = -12$  MeV,  $R = 5.85$  F,  $a = 0.60$  F; and  $R_N = 6.9$  F. The dashed lines result from DW calculations in which  $V_\alpha$  was changed to  $-94$  MeV and all other parameters were held the same. The calculated curves are arbitrarily normalized to the data.

excited states are resolved. The second-excited state is partially obscured by the alpha group from the  $\text{Fe}^{58}(\text{He}^3, \alpha)\text{Fe}^{57}$  ground-state reaction, which appears because of the  $\text{Fe}^{58}$  contaminant in the target. The second-excited state peak and the contaminant peak were analyzed together because of the difficulty of unfolding the two peaks with the limited statistics of the data. The absolute cross section was corrected for the contaminant contribution; the correction was approximately 10% throughout the angular region investigated. The higher excited states, as indicated from the level diagram (Fig. 1), form a complex, multiple-peaked group structure that could not be meaningfully analyzed.

The angular distributions for the ground-, first-excited,

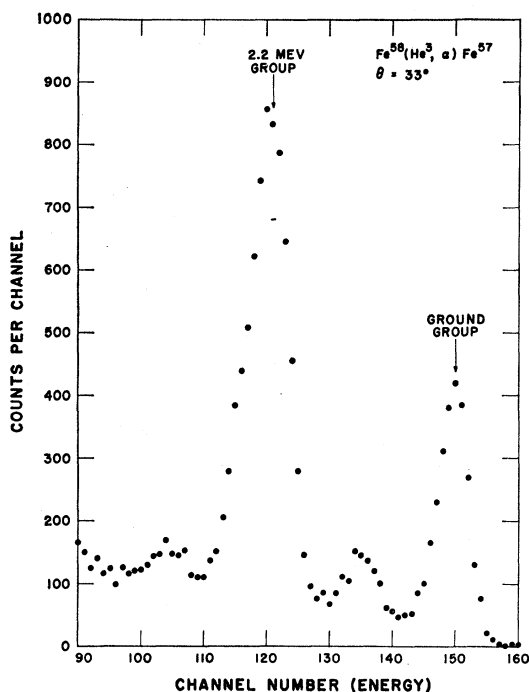


FIG. 7. Energy spectrum of alpha particles from the  $\text{Fe}^{58}(\text{He}^3, \alpha)\text{Fe}^{57}$  reaction at  $\theta_{\text{lab}} = 33^\circ$ .

and second-excited states are shown in Fig. 6. The ground-state distribution shows the characteristics of an  $l=1$  angular-momentum transfer, while the first- and second-excited states show the characteristics of an  $l=3$  transfer.

The most striking feature of the  $\text{Fe}^{57}(\text{He}^3, \alpha)\text{Fe}^{56}$  angular distributions is their low cross section relative to the  $\text{Fe}^{56}(\text{He}^3, \alpha)\text{Fe}^{55}$  distributions. The cross section of the  $\text{Fe}^{57}(\text{He}^3, \alpha)\text{Fe}^{56}$  ground-state distribution is approximately 1/100 that of the  $\text{Fe}^{56}(\text{He}^3, \alpha)\text{Fe}^{55}$  ground- and first-excited state distribution. This ratio can be compared to the results of the  $(d, t)$  experiment of Zeidman *et al.*, which yielded a ratio of  $\frac{1}{5}$  for the equivalent transitions. Similarly, the  $(\text{He}^3, \alpha)$  transition to the first excited state of  $\text{Fe}^{56}$  proceeds with a cross section about  $\frac{1}{10}$  that to be expected on the basis of the  $(d, t)$  experiment. Comparison of the  $(\text{He}^3, \alpha)$  data to the  $(p, d)$  data of Goodman *et al.* yields approximately the same ratios for these sets of transitions as those obtained in the comparison to the  $(d, t)$  data. The  $(\text{He}^3, \alpha)$  transition to the second-excited state of  $\text{Fe}^{56}$  cannot be compared to the  $(d, t)$  results, since this transition could not be analyzed by Zeidman *et al.*, but it has a cross section substantially lower than that expected on the basis of the  $(p, d)$  experimental results.

In addition to the low cross sections observed, the suppression of  $l=1$  transitions relative to  $l=3$  transitions, when compared to the analogous  $(d, t)$  transitions, again appears in the  $\text{Fe}^{57}(\text{He}^3, \alpha)\text{Fe}^{56}$  reaction. To determine whether this feature might be due to the particular  $\text{He}^3$  energy chosen, the  $\text{Fe}^{57}(\text{He}^3, \alpha)\text{Fe}^{56}$  reaction

was partially investigated with 25-MeV  $\text{He}^3$  particles. At the higher energy, the absolute cross section had increased by approximately a factor of 5; however, the relative  $l=1$  to  $l=3$  cross-section ratio was approximately the same as at the lower energy. The general characteristics of the angular distributions at the higher energy were also similar to those at the lower energy. It was concluded that the differences between the  $(\text{He}^3, \alpha)$  and  $(d, t)$  measurements with regard to the  $l=1$  and  $l=3$  transitions were not due to the particular energy chosen for this work. Because no other isotopes were investigated at the higher  $\text{He}^3$  energy, no comparison of absolute cross-section behavior can be made for different energies.

### C. $\text{Fe}^{58}(\text{He}^3, \alpha)\text{Fe}^{57}$ Reaction

The ground-state  $Q$  of the  $\text{Fe}^{58}(\text{He}^3, \alpha)\text{Fe}^{57}$  reaction is 10.55 MeV. The energy distribution for alpha particles from this reaction at a laboratory scattering angle of  $33^\circ$  is shown in Fig. 7. The ground and 2.2-MeV groups did not maintain a Gaussian shape throughout the angular region investigated and were analyzed for area by adding up the counts under the peaks.

The angular distributions for the two strong groups are shown in Fig. 8. The modest oscillatory structure and forward peaking indicate that each corresponds predominantly to an  $l=3$  orbital angular momentum transfer. The sharp break at  $40^\circ$  in the ground-group angular distribution is probably due to the mixing of

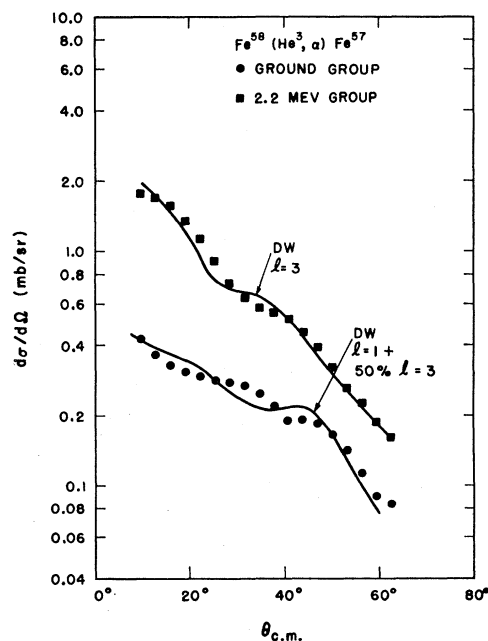


FIG. 8. Angular distributions for the  $\text{Fe}^{58}(\text{He}^3, \alpha)\text{Fe}^{57}$  reaction to the ground group and 2.2-MeV group. The laboratory energy of the  $\text{He}^3$  beam was  $14.40 \pm 0.15$  MeV. The solid lines result from DW calculations using the same parameter values as in Fig. 4, except that  $R=6.5$  F and 5.9 F for the  $\text{He}^3$  well and the alpha well, respectively. Normalization to the data is arbitrary.

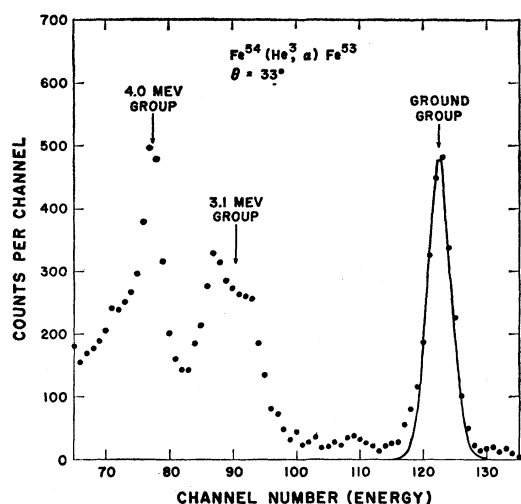


FIG. 9. Energy spectrum of alpha particles from the  $\text{Fe}^{54}(\text{He}^3, \alpha)\text{Fe}^{53}$  reaction at  $\theta_{\text{lab}} = 33^\circ$ . The curve through the datum points is the best fit to the ground group computed by the data analysis code.

$l=1$  with  $l=3$ , and an attempt to fit this shape by mixing the theoretical curves will be discussed later. The group at approximately 1.2 MeV (see Fig. 7) was too weak to be analyzed as dependably as the ground and 2.2-MeV groups, and its angular distribution is not included in Fig. 8.

#### D. $\text{Fe}^{54}(\text{He}^3, \alpha)\text{Fe}^{53}$ Reaction

The ground-state  $Q$  for the  $\text{Fe}^{54}(\text{He}^3, \alpha)\text{Fe}^{53}$  reaction is 7.23 MeV. The energy distribution for alpha particles from this reaction at a laboratory scattering angle of  $33^\circ$  is shown in Fig. 9. The energy spectra maintained the general shape shown in Fig. 9 throughout the angular region investigated, and the three groups analyzed are indicated. The multiple structure of the 3.1-MeV group is apparent, and the 4-MeV group also shows considerable distortion from a Gaussian shape. The 3.1- and 4-MeV groups were analyzed by adding up the counts under the peaks. Owing to the relatively low  $Q$  of the reaction, and the necessity for using at small scattering angles the detection method employing total absorption of elastically scattered  $\text{He}^3$  particles (as described in the Experimental Procedure), data for the reaction to the two excited groups were not obtained for  $\theta_{\text{lab}} < 33^\circ$ .

The angular distributions of the three groups are shown in Fig. 10. The forward peaking and oscillatory structure, when compared to the distributions from the other isotopes, indicate that the groups correspond predominantly to  $l=3$  angular momentum transfers.

#### E. 14-MeV $(d, t)$ Measurements

The distinct contrast between the results of the present  $(\text{He}^3, \alpha)$  experiment and the previous  $(d, t)$  and

$(p, d)$  experiments has been noted. As a check on our experimental techniques, detection equipment, and target composition, we studied the  $(d, t)$  reaction at a deuteron energy of 14 MeV, with  $\text{Fe}^{56}$ ,  $\text{Fe}^{57}$ , and  $\text{Fe}^{58}$  targets. The 14-MeV results were generally similar to those obtained at 20 MeV. Hence, we conclude that the differences between the  $(\text{He}^3, \alpha)$  pickup reaction and the  $(d, t)$  and  $(p, d)$  pickup reactions are basic to the reaction mechanisms.

The triton energy spectrum for the  $\text{Fe}^{58}(d, t)\text{Fe}^{57}$  reaction at a laboratory scattering angle of  $35^\circ$  is shown in Fig. 11. The improved energy resolution of the Au surface barrier detector allowed the 0.36-MeV state to be completely resolved, whereas it could not be analyzed in the experiments of Macfarlane *et al.* and Goodman *et al.* The ground group and the higher energy groups correspond to mixture of several levels.

The great difference in the relative strengths of  $l=1$  and  $l=3$  transitions in the  $(\text{He}^3, \alpha)$  and the  $(d, t)$  reactions is again apparent in the case of the  $\text{Fe}^{58}$  target. In the  $(\text{He}^3, \alpha)$  experiment, the ground-group angular distribution is predominantly  $l=3$  in character (see Fig. 8) from the transition to the  $\frac{5}{2}^-$  0.14-MeV level. In the present  $(d, t)$  experiment, the ground-group angular

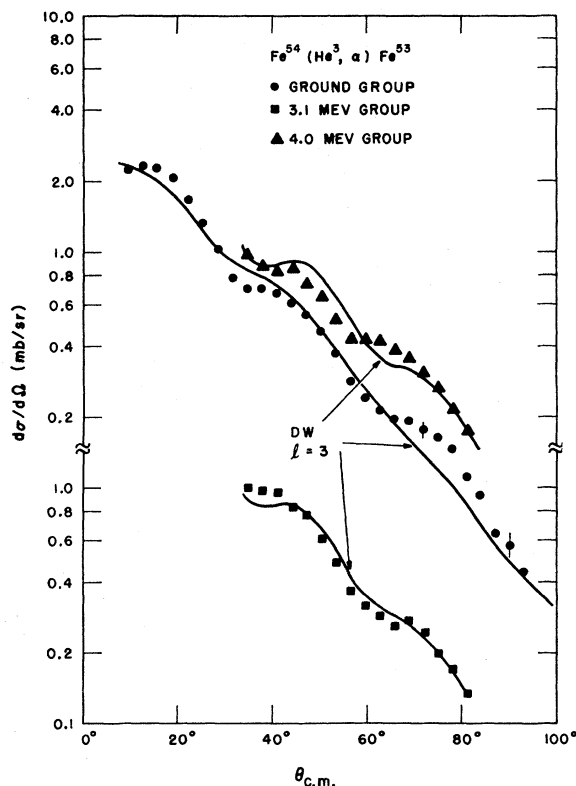


FIG. 10. Angular distributions for the  $\text{Fe}^{54}(\text{He}^3, \alpha)\text{Fe}^{53}$  reaction to the ground, 3.1-MeV, and 4.0-MeV groups. The laboratory energy of the  $\text{He}^3$  beam was  $14.30 \pm 0.15$  MeV. The solid lines result from DW calculations using the same parameter values as in Fig. 4, except that  $R=6.3$  F and 5.7 F for the  $\text{He}^3$  well and the alpha well, respectively. Normalization to the data is arbitrary.

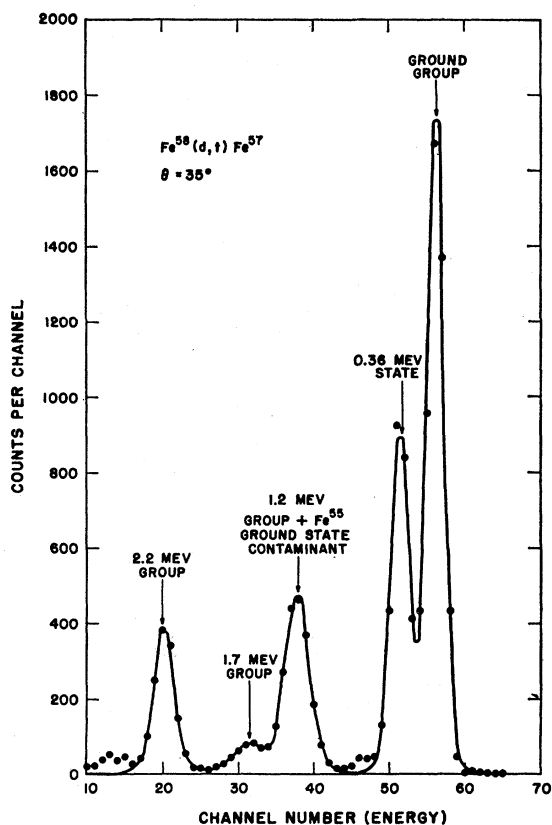


FIG. 11. Energy spectrum of tritons from the  $\text{Fe}^{56}(d,t)\text{Fe}^{57}$  reaction at  $\theta_{\text{lab}} = 35^\circ$ . The curve through the datum points is the best fit computed by the data analysis code.

distribution indicates that the  $l=1$  transitions to the  $\frac{1}{2}^-$  ground state and  $\frac{3}{2}^-$  0.14-MeV state predominate. The details of the angular distribution provide evidence of a small admixture of  $l=3$ , but the amount is too small to be accurately determined. The  $(d,t)$  work of Macfarlane *et al.* agrees with this result.

#### IV. DISCUSSION

The difficulties which might be experienced when treating  $(\text{He}^3, \alpha)$  reaction angular distributions with a PW analysis have been discussed in the Introduction. It was seen in the Results that the  $(\text{He}^3, \alpha)$  data differed considerably from the  $(d,t)$  and  $(p,d)$  data with regard to the relative intensities of  $l=1$  and  $l=3$  angular distributions, and also with regard to the relative magnitudes of the cross sections for the  $\text{Fe}^{57}$  and the  $\text{Fe}^{56}$  targets. In this section, we shall make quantitative comparisons between the results of PW analyses of the  $(\text{He}^3, \alpha)$  data and the  $(d,t)$  data, in order to illustrate the inadequacy of a PW treatment of the  $(\text{He}^3, \alpha)$  reaction. Following this, we shall discuss the application of DW calculations to the  $(\text{He}^3, \alpha)$  data. The results of the DW calculations will then be compared to the results of the PW analysis of the  $(d,t)$  data and the DW analysis of the  $(p,d)$  data. Ideally, DW calculations should be

made for the  $(d,t)$  reaction also. In the present paper, this is not done, and we rely upon the PW analysis; a large body of information has been collected which attests to the self-consistency and usefulness of PW calculations for  $(d,t)$  data such as those with which we are concerned.<sup>1</sup>

#### A. Plane-Wave Analysis

In the  $\text{Fe}^{56}(d,t)\text{Fe}^{55}$  experiments of the Argonne group,<sup>8,9</sup> the sum of  $\Theta^2$  obtained for the  $l=1$  transitions to the ground- and first-excited states of  $\text{Fe}^{55}$  was  $\sum \Theta^2(1) = 5.2$ , and for the  $l=3$  transition to the 1.4-MeV group was  $\sum \Theta^2(3) = 2.7$ . The ratio of these numbers is  $\sum \Theta^2(1)/\sum \Theta^2(3) = 1.9$ . In the  $(\text{He}^3, \alpha)$  reaction,  $l=3$  transitions are enhanced relative to  $l=1$  transitions, as noted earlier, and to a good approximation the distribution of the alpha particles from the 1.4-MeV group of  $\text{Fe}^{56}$  shows only the  $l=3$  character. (See Figs. 3 and 4.) An  $l=3$  PW calculation can be normalized to the 1.4-MeV group distribution at  $10^\circ$ , near the maximum of the distribution. An  $l=1$  curve can be normalized at its second maximum to the  $24^\circ$  maximum of the ground- and first-excited state distribution. (Both curves require a cutoff radius  $r_0 = 5.0$  F.) The ratio of the numbers extracted by this procedure is  $\sum \Theta^2(1)/\sum \Theta^2(3) = 0.32$ , in disagreement with the ratio of 1.9 obtained from the  $(d,t)$  reaction analysis.

The normalization procedure used above in the  $l=1$  case for the  $(\text{He}^3, \alpha)$  reaction is quite arbitrary. Usually, when  $l=1$  PW curves are fitted to  $(d,t)$  and  $(d,p)$  distributions at the first maximum, the predicted second maximum falls below the experimental second maximum. In the present case, decreasing the magnitude of the PW curve in accordance with this observation only serves to increase the discrepancy between the  $(\text{He}^3, \alpha)$  and the  $(d,t)$  results.

If PW fits were made to the second experimental maximum of two different  $l=1$   $(\text{He}^3, \alpha)$  angular distributions, the ratio of the extracted numbers  $\Theta^2$  might be meaningful. For example, the Argonne group used this method in the analysis of their  $(d,t)$  data. They were able to obtain experimentally the first peak of the  $\text{Fe}^{56}(d,t)\text{Fe}^{55}$  ground-state angular distribution, and a PW fit to this peak yielded a predicted second maximum which fell at the position of the experimental second maximum, but had about half its magnitude. On the other hand, the angular distribution of tritons from the  $\text{Fe}^{57}(d,t)\text{Fe}^{56}$  ground-state reaction had shifted toward smaller angles, owing to the relatively high  $Q$  of the reaction, and the usual primary peak was not observed. Zeidman *et al.* assumed that since the energy of tritons from the  $\text{Fe}^{56}$  ground state was only 3.5 MeV higher than that of tritons from the  $\text{Fe}^{55}$  ground state, it was reasonable to assign the same ratio of second maximum to first maximum as in the  $\text{Fe}^{56}(d,t)\text{Fe}^{55}$  ground-state reaction. The  $\text{Fe}^{57}(d,t)\text{Fe}^{56}$  ground-state reduced width was therefore obtained by normalizing the second

maximum of a PW calculation at half the cross section of the experimental maximum of the angular distribution. It is estimated that the error introduced by this extrapolation procedure does not exceed 20%.<sup>8</sup> It will now be shown that a second-maximum analysis of the analogous ( $\text{He}^3, \alpha$ ) transition yields a much different ratio of the extracted numbers  $\Theta^2$ .

The PW analysis of the  $\text{Fe}^{57}(d, t)$  experiment by Zeidman *et al.* yielded  $\Theta^2(1) = 1.1$  for the  $l=1$  transition to the ground state of  $\text{Fe}^{56}$ , compared to  $\sum \Theta^2(1) = 5.2$  for the  $\text{Fe}^{56}(d, t)$   $l=1$  transitions to the ground- and first-excited states of  $\text{Fe}^{55}$ .<sup>8</sup> The ratio of these two numbers is 0.21. For the  $\text{Fe}^{57}(\text{He}^3, \alpha)\text{Fe}^{56}$  reaction, a PW analysis of the ground-state distribution may be made in a manner similar to that of the  $\text{Fe}^{56}(\text{He}^3, \alpha)\text{Fe}^{55}$  ground- and first-excited state distribution, i.e., the second maximum of an  $l=1$  calculation is fit to the maximum of the experimental ground-state distribution near  $13^\circ$ . (See Fig. 6.) A cutoff radius of 5.0 F is required, just as in the  $\text{Fe}^{56}(\text{He}^3, \alpha)\text{Fe}^{55}$  case. The ratio of the two values of  $\Theta^2$  obtained in this manner is 0.010, to be compared to 0.21 from the  $(d, t)$  experiment—a factor of 21 between the analyses of the two reactions.

## B. Distorted-Wave Analysis

If the values of the optical model parameters required to fit elastic scattering distributions are known, the DW theory, if valid, should predict, for the same parameter values, angular distributions similar to those observed for the corresponding nuclear reaction. Actual DW calculations will yield less accurate predictions, owing to additional approximations introduced in the calculations. The DW numerical calculations of the present experiment were made with the code developed at the Rice Institute by W. R. Gibbs and W. Tobocman and adapted for the Los Alamos IBM 704 and 7090 computers by Blair Swartz, L. S. Rodberg, and W. S. Hall. This code employs Woods-Saxon type wells for both real and imaginary optical potentials, zero-range forces, and other simplifications. It has, however, had success in the interpretation of  $(d, p)$  angular distributions,<sup>2,6,18</sup> and the required parameter values are usually in the neighborhood of those required for good optical model fits to elastic-scattering data.

New calculations have recently been made<sup>3,19</sup> which incorporate more sophisticated features (e.g., spin-orbit forces, surface absorption, finite range of interaction), and should yield improved predictions.

### a. Optical Model Fits to Elastic Data

Figure 12 shows the angular distributions for  $14.41 \pm 0.15$ -MeV  $\text{He}^3$  particles and  $26.45 \pm 0.15$ -MeV alpha particles elastically scattered from  $\text{Fe}^{56}$ . In

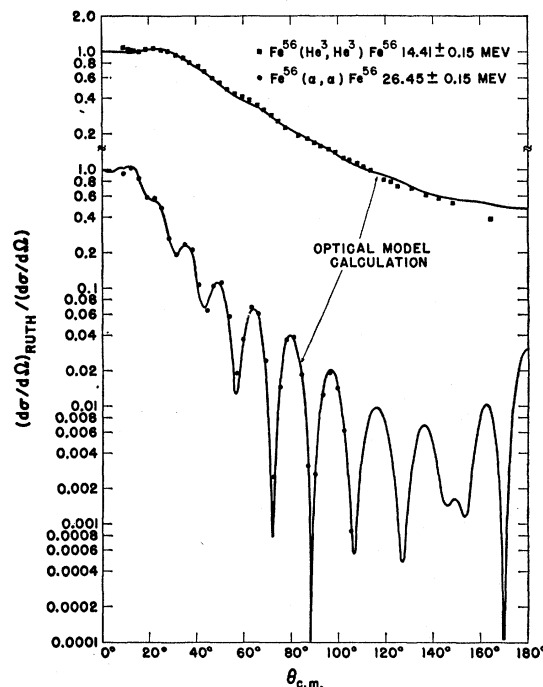


FIG. 12. Angular distributions for  $\text{He}^3$  and alpha particles elastically scattered from  $\text{Fe}^{56}$ . The solid lines result from optical model numerical calculations. The parameters used in the  $\text{He}^3$  calculation are  $V = -32$  MeV,  $W = -13$  MeV,  $R = 6.4$  F,  $a = 0.58$  F. The parameters used in the alpha calculation are  $V = -74$  MeV,  $W = -13$  MeV,  $R = 5.85$  F, and  $a = 0.60$  F.

the  $\text{He}^3$  case, the search for an optical model fit was begun with parameter values near those suggested by the work of Aguilar *et al.*<sup>20</sup> and Greenlees *et al.*,<sup>21</sup> who studied the elastic scattering of  $\text{He}^3$  particles from selected isotopes at energies of approximately 29 MeV. At 14.4 MeV, the structure of the  $\text{He}^3$  distribution on  $\text{Fe}^{56}$  has been reduced from that which appears for neighboring isotopes at 29 MeV, but has not disappeared entirely. The solid line in Fig. 12 is the best calculated fit by visual inspection to the experimental  $\text{He}^3$  angular distribution; the parameter values are given in the caption. The real part of the Saxon potential  $V$ , the diffuseness parameter  $a$ , and the well radius  $R$  all have values close to those suggested by the 29-MeV work. It was necessary to change the imaginary part of the potential well  $W$  from a typical value of  $-25$  MeV at the 29-MeV  $\text{He}^3$  energy to  $-13$  MeV in the present case, in order to approximate the weak oscillatory structure observed in the experimental data. From optical-model analyses of data for elastically scattered alpha particles, it is known that there are several combinations of parameter values which yield equally good optical-model fits to the elastic distribu-

<sup>18</sup> W. R. Gibbs and W. Tobocman, Phys. Rev. **124**, 1496 (1961).

<sup>19</sup> W. R. Gibbs, Ph.D. thesis, Rice University, 1961 (unpublished), and private communication.

<sup>20</sup> J. Aguilar, A. García, J. B. A. England, P. E. Hodgson, and W. T. Toner, Nuclear Phys. **25**, 259 (1961).

<sup>21</sup> G. W. Greenlees, J. S. Lilley, P. C. Rowe, and P. E. Hodgson, Nuclear Phys. **24**, 334 (1961).

tions.<sup>22</sup> In the present study of  $\text{He}^3$  scattering from  $\text{Fe}^{56}$ , it was determined that another parameter region of convergence to the data exists at  $V \approx -68$  MeV,  $R \approx 6.3$  F, but a thorough investigation of the region was not made.

The best optical-model fit by inspection to the data for elastically scattered alpha particles is also shown in Fig. 12 as a solid line through the datum points; the parameter values are given in the figure caption. Another region of convergence was found at  $V \approx -40$  MeV,  $R \approx 6.0$  F, but, as in the  $\text{He}^3$  case, it was not carefully investigated. The results of employing these different parameter values in the DW calculations will be mentioned later, but the predictions were not strikingly different.

### b. $\text{Fe}^{56}(\text{He}^3, \alpha)\text{Fe}^{55}$ Reaction

Figure 4 shows the DW curves obtained for the  $\text{Fe}^{56}(\text{He}^3, \alpha)\text{Fe}^{55}$  reaction to the states analyzed in the present experiment. As was discussed in the Introduction, the present DW calculation does not predict absolute cross sections for the  $(\text{He}^3, \alpha)$  reaction; consequently, the DW curves have been arbitrarily normalized to the experimental data. (The ratios of experimental to predicted cross sections are important, however, and will be used to obtain ratios of spectroscopic factors.) The  $\text{He}^3$  parameters were held at those values required for the optical-model fit to the elastic-scattering data. Because the final reaction system consists of an alpha particle and a residual  $\text{Fe}^{55}$  nucleus, the value of  $R_\alpha$  was decreased by 0.05 F from the  $\text{Fe}^{56}$  elastic scattering, in approximate agreement with an  $A^{1/3}$  dependence. The value of  $a$ , the diffuseness parameter, was held the same as for the elastic scattering, and  $V_\alpha$  and  $W_\alpha$  were adjusted to give the best fit to the ground- and first-excited state distribution. The curves shown in Fig. 4 were obtained by using the values  $V_\alpha = -79$  MeV,  $W_\alpha = -12$  MeV, as opposed to the elastic-scattering values of  $V_\alpha = -74$  MeV,  $W_\alpha = -13$  MeV. A 2-MeV change in  $V_\alpha$  produces a shift of about a degree in the position of the maximum at  $50^\circ$ , alters slightly the shape of the curve, and changes the predicted cross section by a few percent. A 1-MeV change in  $W_\alpha$  does not shift the angular positions of the maxima or affect the normalization ratio appreciably, but it does change the maxima-to-minima ratios by a few percent.

The fact that the best fit to the  $\text{Fe}^{56}(\text{He}^3, \alpha)\text{Fe}^{55}$  ground- and first-excited state distribution was achieved with only small changes in  $V_\alpha$  and  $W_\alpha$  from their values for the elastic scattering supports the validity of the DW calculation for the  $(\text{He}^3, \alpha)$  reaction. The results are especially encouraging when one considers that for neutron and proton scattering in this energy region, the real part of the optical well increases in absolute magnitude and the imaginary part decreases in absolute magnitude as the energy of the incident alpha particles

is decreased.<sup>23</sup> In the present experiment, the c.m. energy of the final system in the  $\text{Fe}^{56}(\text{He}^3, \alpha)\text{Fe}^{55}$  ground-state reaction is approximately 2 MeV lower than for the elastic scattering.

The value of  $R_N$ , the radius parameter, at which the inside and outside neutron wave functions are matched, was arbitrarily held at 6.9 F throughout all of the DW calculations. Changing the value results in a slightly different shape and average slope of the calculated curve, but the main effect is a large change in the predicted absolute cross section. An increase in  $R_N$  of 0.5 F raises the absolute cross section scale by approximately 50%. It is possible that  $R_N$  should be chosen somewhat differently for neutrons from different subshells (e.g.,  $2p$  and  $1f$ ), but there is little evidence on this subject. There is evidence from  $(d, p)$  studies that the value of  $R_N$  should be somewhat larger than the deuteron and proton well radii, and some theoretical justification for this tendency exists.<sup>3</sup> Thus, the value of 6.9 F is in accord with previous work. It is likely that a different value of  $R_N$  would be required for a fit to the data in a calculation which included the effects of finite-range forces, because of the dependence on  $R_N$  of the slope of the calculated curve.

While the reaction to the ground- and first-excited states of  $\text{Fe}^{55}$  involves a single  $l$ -transfer value, namely  $l=1$ , the reaction to the 0.93- and 1.4-MeV group includes both  $l=1$  and  $l=3$  transitions. In comparing the angular distribution of this group to DW predictions, one should therefore sum  $l=1$  and  $l=3$  DW curves in the correct proportion and compare the resultant curve.

It is convenient at this point to introduce the quantity  $S$ , where

$$S = C^2 s. \quad (3)$$

The sum  $\sum S$  corresponds to the combined strength of transitions to an appropriately chosen group of levels. (See, e.g., Macfarlane *et al.*<sup>8</sup>) The measured quantity  $\Theta^2 = C^2 A \theta^2$  thus becomes, from Eqs. (2) and (3),

$$\Theta^2 = S A \theta_0^2. \quad (4)$$

The values of  $\Theta^2$  for the  $l=1$  and  $l=3$  transitions to the 1.4-MeV group of  $\text{Fe}^{55}$  are known from the work of the Argonne group; the value of  $\Theta^2$  for the  $l=3$  transition to the 0.93-MeV state can be estimated from the present  $(d, t)$  experiment and from the data of Zeidman *et al.* to be approximately 20% of the value for the  $l=3$  transition to the 1.4-MeV group. From Eq. (4), using the values of  $\Lambda \theta_0^2(1)$  and  $\Lambda \theta_0^2(3)$  determined by Macfarlane *et al.*, one obtains the small ratio  $\sum S(1)/\sum S(3) = 0.06$  from the PW analysis of the  $(d, t)$  reaction to the 0.93- and 1.4-MeV group. The DW calculation assumes the transfer of a nucleon with the full single-particle reduced width and unit value for  $C^2$ , i.e.,  $S$  has

<sup>23</sup> F. Bjorklund, *Proceedings of the International Conference on the Nuclear Optical Model* (Florida State University, Tallahassee, 1959), pp. 1-15.

<sup>22</sup> G. Igo, *Phys. Rev.* **115**, 1665 (1959).

TABLE I. Values of  $S$  from DW analysis of the ( $\text{He}^3, \alpha$ ) reaction, PW analysis of the ( $d, t$ ) reaction, and DW analysis of the ( $p, d$ ) reaction. All values are given relative to the sum  $\sum S_\sigma$  for the reaction to the  $\text{Fe}^{56}$  ground- and first-excited states.

Target	Final level (MeV)	$l$ transfer	( $\text{He}^3, \alpha$ ) DW analysis $S/\sum S_\sigma$	( $d, t$ ) PW analysis <sup>a</sup> $S/\sum S_\sigma$	( $p, d$ ) DW analysis <sup>b</sup> $S/\sum S_\sigma$
$\text{Fe}^{56}$	$\text{Fe}^{56} \ 0.93 + 1.4^c$	1	d	0.076	
		3	2.1	1.3 <sup>e</sup>	4.1 <sup>e</sup>
		3	0.6		1.6
$\text{Fe}^{57}$	$\text{Fe}^{56} \ 0$	1	0.077	0.21	0.081
		1	d	0.42	0.45
		3	0.39	0.59	
$\text{Fe}^{58}$	$\text{Fe}^{57} \ 0^e$	3	0.042	0.069	0.17
		1	1.9	2.1	1.2
		3	0.97	<0.8	
$\text{Fe}^{54}$	$\text{Fe}^{53} \ 0^e$	1	1.0 <sup>f</sup>	0.67	0.69
		3	0.11 <sup>f</sup>	<0.2	
		3	2.5	1.7	4.7
$\text{Fe}^{54}$	$\text{Fe}^{53} \ 0^e$	3	1.9	1.2	4.3
		3	1.8		
		3	2.0		

<sup>a</sup> The ratios in this column are obtained from reference 8, except for the transition to the  $\text{Fe}^{56} \ 2.09$ -MeV level, for which the ratio comes from the present ( $d, t$ ) experiment.

<sup>b</sup> The ratios in this column are obtained from reference 7.

<sup>c</sup> This is not a resolved level but a group of levels.

<sup>d</sup> The  $l=1$  contribution to the angular distribution was too weak to be properly analyzed.

<sup>e</sup> This value has been increased 20% from the value for the transition to the 1.4-MeV group, to approximate the inclusion of the 0.93-MeV transition.

<sup>f</sup> This ratio may be in error by as much as a factor of 2.

unit value in the calculation. In Fig. 4, the  $l=1$  and  $l=3$  DW curves calculated for the ( $\text{He}^3, \alpha$ ) reaction to the 0.93- and 1.4-MeV group have therefore been added together in the ratio of 6% to 100% of the predicted magnitudes, respectively, and the result has been normalized to the experimental curve. As will be shown later in detail, the DW calculation correctly predicts the enhancement of  $l=3$  transitions relative to  $l=1$  transitions. As a result, the addition of 6% of the  $l=1$  calculation contributes only approximately 1% to the magnitude of the final curve at  $10^\circ$ , and a maximum amount of approximately 15% at  $100^\circ$ , and hence does not markedly affect the shape of the curve or its normalization.

The same parameter values were used in the DW calculations for the 0.93- and 1.4-MeV group transitions as for the ground- and first-excited state transitions. Because of the difference in alpha-particle energies, it is probable that one or more of the alpha-particle parameters will have slightly different values for the two sets of transitions. A small change in parameter values could yield a more favorable comparison to the shape of the experimental curve, but would not change the normalization significantly.

The same parameter values were also used in the calculation for the distribution from the 3-MeV group. Very little  $l=1$  admixture is apparent in this distribution, and it was fitted with a pure  $l=3$  calculation.

The effect of changing the parameter values over a wide range was examined. When values from the other regions of convergence to the elastic data (as discussed earlier) were used in the DW calculation, no striking differences resulted. That is, the predicted peak positions and curve structure were about the same; the ratio between magnitudes for  $l=1$  and  $l=3$  distributions

remained about the same; and the cross sections did not change by more than approximately 30% or 40%. However, when parameter values other than those required for optical-model fits to the elastic data were used, good fits to the  $\text{Fe}^{56}(\text{He}^3, \alpha)\text{Fe}^{55}$  angular distributions were not obtained.

Ratios of  $S$  values between one transition and another can be obtained from the normalization of DW curves to experimental angular distributions. These ratios may then be compared to the ratios obtained from PW and DW analyses of the comparable transitions from ( $d, t$ ) and ( $p, d$ ) reactions, respectively. For the  $\text{Fe}^{56}(\text{He}^3, \alpha)\text{Fe}^{55}$  reaction to the 0.93- and 1.4-MeV group relative to the reaction to the ground- and first-excited states, the normalization of the DW calculations to the data yields the ratio  $\sum S(3)/\sum S_\sigma = 2.1$ . This is in fair agreement with the ratio  $\sum S(3)/\sum S_\sigma = 1.3$  from the PW analysis of the ( $d, t$ ) reaction to the same states.<sup>8</sup> The agreement is slightly poorer between the present results and the ratio of  $\sum S(3)/\sum S_\sigma = 4.1$  obtained from the DW analysis of the ( $p, d$ ) experiment.<sup>7</sup>

In Table I are recorded the ratios obtained from the DW analysis of the ( $\text{He}^3, \alpha$ ) data and, where they exist, the PW analysis of the ( $d, t$ ) data and the DW analysis of the ( $p, d$ ) data.

### c. $\text{Fe}^{57}(\text{He}^3, \alpha)\text{Fe}^{56}$ Reaction

The initial attempt at fitting the  $\text{Fe}^{57}(\text{He}^3, \alpha)\text{Fe}^{56}$  angular distributions with DW calculations was made for the  $l=1$  ground-state transition, with the same parameter values determined from the  $\text{He}^3$  and alpha particle elastic-scattering optical-model fits to  $\text{Fe}^{56}$ . (The radius of the  $\text{Fe}^{57}\text{-He}^3$  optical well was increased by 0.05 F from the  $\text{Fe}^{56}$  value to allow for the increase in the atomic weight.) Two notable effects appeared in the result: The cross section predicted by the calculation was approximately one-fifth that predicted for the  $l=1$  ground-state transition of the  $\text{Fe}^{56}(\text{He}^3, \alpha)\text{Fe}^{55}$  reaction, and the predicted maxima fell approximately  $12^\circ$  from the experimental maxima. The first effect is in the direction that accords with the low cross section found experimentally for the  $\text{Fe}^{57}(\text{He}^3, \alpha)\text{Fe}^{56}$  ground-state reaction, and arises from the calculation solely because of the  $Q$  difference of 3.5 MeV between the  $\text{Fe}^{57}(\text{He}^3, \alpha)\text{Fe}^{56}$  and the  $\text{Fe}^{56}(\text{He}^3, \alpha)\text{Fe}^{55}$  reactions. The discrepancy in the predicted maximal positions may be caused by the high energy of the alpha particles (2.5 MeV higher than that in the elastic scattering) which may require the use of different alpha parameter values; or it may be due to the need for different parameter values for the  $\text{Fe}^{57}\text{-He}^3$  system.

Data on the elastic scattering of  $\text{He}^3$  from  $\text{Fe}^{57}$  are not available at present, and the energy dependence of the alpha parameters is not known. To shift the positions of the predicted maxima of the ground-state distribution, other parameter values were arbitrarily held fixed while the value of  $V_\alpha$  was changed. The solid lines in

Fig. 6 show the calculated angular distributions when  $V_\alpha = -85$  MeV, for which the fit to the ground-state distribution is good. A calculation with  $V_\alpha = -63$  MeV (not shown) also yields a curve with its maxima in the proper positions for the ground-state distribution, but the maximum-to-minimum ratio is not so satisfactory.

From the results of the calculation shown by the solid line in Fig. 6, the ratio of  $S$  for the  $\text{Fe}^{57}(\text{He}^3, \alpha)\text{Fe}^{56}$  ground-state transition to  $\sum S$  for the  $\text{Fe}^{56}(\text{He}^3, \alpha)\text{Fe}^{55}$  ground- and first-excited state transitions is 0.077. (Approximately the same ratio is obtained when the curve calculated for  $V = -63$  MeV is normalized to the data.) This ratio is in only fair agreement with the value of 0.21 obtained from the PW analysis of the  $(d, t)$  work of Zeidman *et al.*, but is in much better agreement than is the value of 0.010 which results from a PW analysis of the same  $(\text{He}^3, \alpha)$  data, as discussed earlier; it is in excellent agreement with the value of 0.081 from the  $(p, d)$  analysis of Goodman *et al.* The present result may be regarded as a further success of the DW calculation for the  $(\text{He}^3, \alpha)$  reaction.

For the  $(\text{He}^3, \alpha)$  reaction to the 0.85-MeV level in  $\text{Fe}^{56}$ ,  $l=3$  and  $l=1$  curves from the DW calculation with  $V_\alpha = -85$  MeV were added together in various proportions in an attempt to reproduce the experimental distribution. The solid line for this transition in Fig. 6 shows the result of adding the calculated curves in the  $l=3$  to  $l=1$  ratio of 100:55, in approximate agreement with the analysis results of the Argonne group. The fit to the experimental data is poor, and cannot be improved significantly by changing the  $l$  ratio. The contribution of the  $l=1$  curve to the sum curve shown is small at small angles, e.g., 5% at  $10^\circ$ , and reaches a maximum of about 60% at  $65^\circ$ . A better fit to the data is shown by the dashed curve in Fig. 6, which is composed of  $l=1$  and  $l=3$  curves calculated with  $V_\alpha = -94$  MeV and summed in the same ratio as for the solid curve. A curve (not shown) similar in structure to the dashed curve, with its maxima properly located, but with a slope somewhat steeper than that of the data, was obtained with  $V \approx -70$  MeV.

The calculation for the reaction to the  $\text{Fe}^{56}$  2.09-MeV state also yields a poor fit to the data with  $V_\alpha = -85$  MeV, and an improved fit with  $V_\alpha = -94$  MeV, as shown by the dashed line. A calculation with  $V_\alpha \approx -74$  MeV yielded a curve (not shown) with its maxima in the desired locations, but with a slope steeper than that of the data. The ground-state distribution is not fitted by the calculation for which  $V_\alpha = -94$  MeV, as shown by the dashed line.

The ratios of  $S$  determined from the normalization of the calculated curves to the data ( $V_\alpha = -85$  MeV for the  $\text{Fe}^{56}$  ground-state calculation and  $V_\alpha = -94$  MeV for the 0.85-MeV and the 2.09-MeV state calculations) are given in Table I. These ratios are to be compared to those obtained from the PW analysis of the  $(d, t)$  data and the DW analysis of the  $(p, d)$  data. (The angular distribution of tritons from the 2.09-

MeV state was not obtained by the Argonne group, and for this transition the result of the PW analysis of the present  $(d, t)$  experiment was used.) The ratios for the ground-state transition have already been discussed. For the transitions to the 0.85-MeV state and the 2.09-MeV state, the DW analysis of the  $(\text{He}^3, \alpha)$  data yields ratios which are in somewhat better agreement with the  $(d, t)$  PW ratios than are those for the ground-state transition. The ratio obtained from the DW analysis of the  $(p, d)$  reaction to the 2.09-MeV state is substantially larger than the ratios obtained for the  $(\text{He}^3, \alpha)$  and  $(d, t)$  reactions to that state.

#### d. $\text{Fe}^{58}(\text{He}^3, \alpha)\text{Fe}^{57}$ and $\text{Fe}^{54}(\text{He}^3, \alpha)\text{Fe}^{53}$ Reactions

Figure 8 shows the results of DW calculations for the  $\text{Fe}^{58}(\text{He}^3, \alpha)\text{Fe}^{57}$  reaction. The parameter values are those which were used in the  $\text{Fe}^{56}(\text{He}^3, \alpha)\text{Fe}^{55}$  calculations, with appropriate adjustments in optical-well radii. The  $l=3$  fit to the 2.2-MeV group distribution is quite good. For the ground-group reaction,  $l=1$  and  $l=3$  DW curves calculated with the parameter values given in the figure caption were summed in various ratios. The figure shows the best fit by visual inspection, the result of adding  $l=1$  and  $l=3$  curves approximately in the ratio of 100% to 50% of the predicted magnitudes, respectively. The fit could undoubtedly be improved by slight changes in parameter values, and a somewhat different  $l=1$  to  $l=3$  ratio might then be obtained.

The angular distribution (not shown in Fig. 8) of the weak group at 1.2 MeV (see Fig. 7) was not determined with sufficient reliability to permit an accurate analysis in terms of its  $l=1$  and  $l=3$  components. The ratios of  $S$  values can be estimated as  $\sum S(1)/\sum S_g \approx 1.0$  and  $\sum S(3)/\sum S_g \approx 0.11$ , but these ratios may be in error by as much as a factor of 2.

The ratios of  $S$  values obtained for this reaction, listed in Table I, are in good agreement with the results of the  $(d, t)$  analysis, but in somewhat poorer agreement with the  $(p, d)$  results.

#### e. $\text{Fe}^{54}(\text{He}^3, \alpha)\text{Fe}^{53}$ Reaction

Figure 10 shows the results of DW calculations for the  $\text{Fe}^{54}(\text{He}^3, \alpha)\text{Fe}^{53}$  reaction, again using the same parameter values as for the  $\text{Fe}^{56}(\text{He}^3, \alpha)\text{Fe}^{55}$  reaction calculations, with appropriate adjustments in optical-well radii. The  $l=3$  fits to the data are acceptable.

Very little experimental information is available on the energy-level structure of  $\text{Fe}^{53}$ . The  $\text{Fe}^{54}$  nucleus has 28 neutrons, and the ground state should have very nearly a filled  $f_{7/2}$  neutron shell. If the value of  $\sum S = 1.7$  obtained by Macfarlane *et al.*<sup>8</sup> for the sum of  $(d, t)$  transitions from the  $\text{Fe}^{56}$  ground state to the ground- and first-excited states of  $\text{Fe}^{55}$  is accepted, the present  $\text{Fe}^{54}(\text{He}^3, \alpha)\text{Fe}^{53}$  analysis yields the value  $\sum S = 5.7 \times 1.7 = 9.7$  for the sum of  $f_{7/2}$  transitions. This is close

to the expected value of 8 (the number of neutrons in the closed  $f_{7/2}$  shell), and indicates that all of the important  $f_{7/2}$  transitions have probably been detected. The  $f_{7/2}$  single-hole resonance is thus spread over about 4 MeV, compared to a spread of about 3 MeV observed in the  $V^{51}(d, t)V^{50}$  reaction.<sup>8</sup>

### V. CONCLUSIONS

The ( $\text{He}^3, \alpha$ ) pickup reaction is useful in the study of nuclear spectroscopy because  $l=3$  transitions are strongly enhanced over  $l=1$  transitions, in contrast to the behavior of the analogous ( $d, t$ ) and ( $p, d$ ) pickup reactions. Satchler<sup>24</sup> has investigated likely reasons for the  $l$ -behavior of the ( $\text{He}^3, \alpha$ ) reaction, and suggests a possible explanation based on the concept of the "black" nucleus.<sup>25</sup> According to this concept, incoming partial waves  $L_a$  and outgoing waves  $L_b$  will contribute strongly to a reaction only at  $L_a \approx L_{a0} = k_a R_a$  and  $L_b \approx L_{b0} = k_b R_b$ , respectively, where  $k$  is the wave number and  $R$  is a radius associated with the scattering. Then, since the angular momentum transferred to the nucleus is given by  $\mathbf{l} = \mathbf{L}_a - \mathbf{L}_b$ , reactions with  $l < |L_{a0} - L_{b0}|$  will be inhibited. The greater the difference ( $|L_{a0} - L_{b0}| - l$ ), the stronger will be the inhibition. The term  $L_{a0} - L_{b0}$  may be written as

$$L_{a0} - L_{b0} = 0.22 \{ R_a (\mu_a E)^{1/2} - R_b [\mu_b (E + Q)]^{1/2} \}, \quad (5)$$

where  $\mu$  is the reduced mass and  $E$  is the energy of the initial system.

To examine the behavior of Eq. (5) under the conditions of the present ( $\text{He}^3, \alpha$ ) experiment, we take  $E = 14$  MeV,  $R_a = R_b = 6.5$  F,  $Q = 10$  MeV,  $\mu_a = 3$ , and  $\mu_b = 4$ . Equation (5) then yields the value

$$L_{b0} - L_{a0} = 4.8,$$

so that  $l=4$  or  $l=5$  transitions are greatly favored compared to  $l=0$  or  $l=1$  transitions, in agreement with the experimental results and DW predictions. As the value of  $Q$  is decreased, the difference ( $L_{b0} - L_{a0}$ ) diminishes. At  $Q \approx 0$ , the difference is 1.4, and the strength of the transitions should be approximately "normal," i.e., the cross section should decrease as  $l$  increases. DW calculations with the present code support this conclusion; at  $Q=0$ , the cross section of an  $l=1$  transition has increased and that of an  $l=3$  transition has decreased, relative to the cross sections at  $Q=10$  MeV, so that the  $l=1$  cross section is a factor of 5 higher than the  $l=3$  cross section.<sup>26</sup>

<sup>24</sup> G. R. Satchler (private communication).

<sup>25</sup> N. Austern, Ann. Phys. (New York) **15**, 299 (1961).

<sup>26</sup> A prediction of the relative magnitude of the cross section as a function of the quantity  $|L_{a0} - L_{b0}|$  is in semiquantitative agreement with the observed reduction in cross section of the high- $Q$   $\text{Fe}^{57}(\text{He}^3, \alpha)\text{Fe}^{56}$  reaction.

In contrast to the above results, ( $p, d$ ) and ( $d, t$ ) reactions at 20 MeV with typical values of  $Q$  have a value of  $|L_{a0} - L_{b0}|$  of only 1 or 2, and the  $l$  behavior of these reactions is "normal." Furthermore, in the present ( $\text{He}^3, \alpha$ ) reaction, as the energy  $E$  is changed the difference ( $L_{b0} - L_{a0}$ ) remains approximately constant for a typical  $Q$  of 10 MeV. The prediction is, then, that the  $l$  behavior of the reaction will be approximately the same over a range of energies. The experimental observation that at  $E \approx 25$  MeV, the  $l=1$  to  $l=3$  cross-section ratio has approximately the same value as at  $E \approx 14$  MeV is in accord with this prediction.

In many cases, PW analyses of ( $\text{He}^3, \alpha$ ) angular distributions do not yield useful reaction information. In contrast, DW calculations (with reasonable parameter values) fit the data, and the dependence of the reaction on  $Q$  and  $l$  is correctly predicted. Ratios of spectroscopic factors obtained from the normalization of DW calculations to the angular distributions are usually in fair to good agreement with ratios obtained from PW fits to the corresponding ( $d, t$ ) distributions. It is interesting that the DW analysis of the ( $p, d$ ) data yields ratios of spectroscopic factors which are only in fair over-all agreement with those of the ( $\text{He}^3, \alpha$ ) analysis, and in rather poor agreement, in some cases, with those of the ( $d, t$ ) analysis.

The cross section predicted by the DW calculation for the ( $\text{He}^3, \alpha$ ) reaction is not a strong function of parameter values other than  $R_N$ , the neutron wavefunction matching parameter. Thus, when the potential  $V_a$  was adjusted from the value used for the  $\text{Fe}^{56}(\text{He}^3, \alpha)\text{Fe}^{55}$  reaction to obtain a fit to the data for the  $\text{Fe}^{57}(\text{He}^3, \alpha)\text{Fe}^{56}$  reaction, the ratios of spectroscopic factors obtained are internally consistent to within a few percent.

Except for the absolute cross section, the main features of the ( $\text{He}^3, \alpha$ ) reaction on the Fe isotopes are predicted by the DW calculation. Before the ( $\text{He}^3, \alpha$ ) reaction can be interpreted in detail and fully exploited, more elastic-scattering data, reaction data, and analyses with optical model and DW calculations are required.

### ACKNOWLEDGMENTS

The authors are greatly indebted to D. D. Armstrong for his assistance in the early phases of the experiment, to F. P. Gibson for his aid in the computational program, and to Professor L. S. Rodberg for his many helpful comments and suggestions. We wish to acknowledge valuable correspondence with Dr. G. R. Satchler. We are grateful to Professor D. W. Miller for his critical reading of the manuscript.